⊙termis.

Tissue Engineering
& Regenerative Medicine
International Society

ORIGINAL ARTICLE

Polycistronic Delivery of IL-10 and NT-3 Promotes Oligodendrocyte Myelination and Functional Recovery in a Mouse Spinal Cord Injury Model

Dominique R. Smith, PhD,[1] Courtney M. Dumont, PhD,[1–3] Jonghyuck Park, PhD,[4,5] Andrew J. Ciciriello, MS,[1,2]
Amina Guo, BS,[1] Ravindra Tatineni, BS,[1] Brian J. Cummings, PhD,[6–9]
Aileen J. Anderson, PhD,[6–9] and Lonnie D. Shea, PhD[1,10]

One million estimated cases of spinal cord injury (SCI) have been reported in the United States and repairing an injury has constituted a difficult clinical challenge. The complex, dynamic, inhibitory microenvironment postinjury, which is characterized by proinflammatory signaling from invading leukocytes and lack of sufficient factors that promote axonal survival and elongation, limits regeneration. Herein, we investigated the delivery of polycistronic vectors, which have the potential to coexpress factors that target distinct barriers to regeneration, from a multiple channel poly(lactide-co-glycolide) (PLG) bridge to enhance spinal cord regeneration. In this study, we investigated polycistronic delivery of IL-10 that targets proinflammatory signaling, and NT-3 that targets axonal survival and elongation. A significant increase was observed in the density of regenerative macrophages for IL-10+NT-3 condition relative to conditions without IL-10. Furthermore, combined delivery of IL-10+NT-3 produced a significant increase of axonal density and notably myelinated axons compared with all other conditions. A significant increase in functional recovery was observed for IL-10+NT-3 delivery at 12 weeks postinjury that was positively correlated to oligodendrocyte myelinated axon density, suggesting oligodendrocyte-mediated myelination as an important target to improve functional recovery. These results further support the use of multiple channel PLG bridges as a growth supportive substrate and platform to deliver bioactive agents to modulate the SCI microenvironment and promote regeneration and functional recovery.

Keywords: spinal cord injury, biomaterial, gene therapy, axon elongation, axon myelination

Impact Statement

Spinal cord injury (SCI) results in a complex microenvironment that contains multiple barriers to regeneration and functional recovery. Multiple factors are necessary to address these barriers to regeneration, and polycistronic lentiviral gene therapy represents a strategy to locally express multiple factors simultaneously. A bicistronic vector encoding IL-10 and NT-3 was delivered from a poly(lactide-co-glycolide) bridge, which provides structural support that guides regeneration, resulting in increased axonal growth, myelination, and subsequent functional recovery. These results demonstrate the opportunity of targeting multiple barriers to SCI regeneration for additive effects.

[1]Department of Biomedical Engineering, University of Michigan, Ann Arbor, Michigan.
[2]Department of Biomedical Engineering, University of Miami, Coral Gables, Florida.
[3]Biomedical Nanotechnology Institute at University of Miami (BioNIUM), University of Miami, Miami, Florida.
[4]Department of Pharmaceutical Sciences, College of Pharmacy, University of Kentucky, Lexington, Kentucky.
[5]Spinal Cord and Brain Injury Research Center, University of Kentucky, Lexington, Kentucky.
[6]Institute for Memory Impairments and Neurological Disorders (iMIND), University of California, Irvine, California.
[7]Sue and Bill Gross Stem Cell Research Center, University of California, Irvine, California.
Departments of [8]Anatomy and Neurobiology and [9]Physical Medicine and Rehabilitation, University of California, Irvine, California.
[10]Department of Chemical Engineering, University of Michigan, Ann Arbor, Michigan.

Introduction

NEARLY 17,000 ESTIMATED CASES of spinal cord injury (SCI) occur in the United States each year and repairing an injury to the spinal cord has constituted difficult clinical challenges.[1] Although the spinal cord has some inherent ability to regenerate, the environment that develops post-SCI lacks sufficient factors that promote regeneration and has an abundance of factors that inhibit regeneration. Biomaterial bridges are among strategies to overcome some aspects of the inhibition.[2–8] We have developed multichannel poly(lactide-co-glycolide) (PLG) bridges that support axonal growth and myelination, along with functional recovery. Bridges have an interconnected pore structure that allows infiltration of endogenous cell populations and channels that direct axonal growth into and through the lesion. These bridges are biodegradable and are ultimately replaced by native tissue. We have demonstrated that bridge implantation alone supports some regeneration, yet are insufficient because of complex, dynamic, inhibitory microenvironment.[2,3,5]

The inhibitory environment consists of multiple barriers to nerve regeneration, most notably proinflammatory signaling from invading immune cells and lack of sufficient factors that promote axonal survival and elongation.[9] Analysis of this environment has led to the discovery of the cytokine/neurotrophin axis in axon growth. Cytokines (IL-10, IL-4, IL-6) released by invading macrophages can influence the expression of neurotrophins (NT-3, NT-4, nerve growth factor [NGF]) and their receptors.[10] Macrophages invade the lesion and contribute to both injury and repair.[11] Macrophages exist on a spectrum of activation states ranging from proinflammatory to proregenerative.[12,13] Proregenerative macrophages present enhanced phagocytosis capabilities.[14,15] and can promote tissue regeneration.[11] The proinflammatory/proregenerative ratio can expedite or drastically reduce axonal growth into the lesion site.[16] Combinations of interleukins and neurotrophins have been shown to promote or inhibit neurite extension *in vitro*, although the ability to locally deliver combinations of factors has limited the *in vivo* translation.[10,17]

Traditional strategies for localized delivery of factors to augment the microenvironment involve osmotic pumps that can clog and require surgery for removal or direct injection of factors that are rapidly cleared and lead to off-target effects.[18–20] Furthermore, cell therapy strategies, such as Schwann cells, olfactory ensheathing cells, or neural stem cells, have limited cell survival and engraftment and may require immunosuppression. In addition to providing structural support for regenerating tissue, our bridges are also capable of long-term, localized transgene expression of lentivirus. Previously, single viral vectors have been delivered with positive results, but the multiple barriers to regeneration must be addressed simultaneously to create holistic treatments for SCI. Delivering multiple lentiviruses may result in inactivation or increased immunogenicity. Nonviral strategies, such as naked DNA or lipofection, have a lower efficiency, whereas other viral strategies would lead to distinct expression patterns. These limitations suggest we need an effective way to delivery multiple factors without increased concentrations of lentivirus.

In this study, we investigated polycistronic vectors for coexpression of NT-3 and IL-10 using PLG bridges after acute SCI. Polycistronic vectors negate the limitations of single lentiviral vectors by encoding coexpression of multiple genes by adding ''self-cleaving'' 2A peptide sites between genes. 2A peptides can lead to high levels of downstream protein expression compared with other strategies for multigene coexpression and are small enough to not negatively interfere with the function of the coexpressed genes.[21] IL-10 can alter the phenotype of invading macrophages toward a proregenerative phenotype and lead to improved spinal cord regeneration,[22,23] whereas NT-3 expression can promote neuron survival and axonal elongation.[19] Herein, we investigated the potential for coexpression to influence macrophage phenotypes, axonal elongation and myelination, and source of the myelination at 12 weeks postinjury, with subsequent studies assessing the functional benefits of codelivery. This research builds upon the success of the multiple channel PLG bridges by delivering multiple gene factors that target distinct barriers to regeneration to elucidate synergistic relationships.

Materials and Methods

Virus production and validation

Lentivirus was produced as previously described.[2] In brief, HEK-293FT cells (80–90% confluent; American Type Culture Collection (ATCC), Manassas, VA) were transfected with third-generation lentiviral packaging vectors and pLenti-CMV-Luciferase, pLenti-CMV-hNT3, pLenti-CMV-hIL10, or pLenti-CMV-hIL10/NT3. Plasmids were incubated in OptiMEM (Life Technologies, Carlsbad, CA) with Lipofectamine 2000 (Life Technologies) and then added to cells. After 48 h the supernatant was centrifuged to remove and then incubated with PEG-It (System Biosciences, Palo Alto, CA). Virus was centrifuged, supernatant was removed, and the pellet was resuspended in sterile phosphate-buffered saline (Life Technologies). Virus aliquots were frozen at −80°C until use. Viral titers used throughout the study were 2E9 IU/mL as determined by the Lentivirus qPCR Titer Kit (Applied Biological Materials, Richmond, BC, Canada).

Fabrication of multichannel bridges

Bridges were fabricated using a sacrificial template variation[24] of the gas foaming/particulate leaching technique, as previously described.[19,25] In brief, PLG (75:25 lactide:glycolide; i.v. 0.70–0.90 dL/g; Lactel, Birmingham, AL) was dissolved in dichloromethane (6% w/w) and emulsified in 1% poly (vinyl-alcohol) using a homogenizer (PolyTron 3100; Kinematica AG, Littau, Switzerland) to create microspheres (z-average diameter ∼1 μm). D-sucrose (Sigma-Aldrich), D-glucose (Sigma-Aldrich), and dextran MW 100,000 (Sigma-Aldrich) were mixed at a ratio of 5.3:2.5:1, respectively, by mass. The mixture was caramelized, cooled, and drawn from solution with a Pasteur pipette to make sugar fibers. Fibers were drawn to 150–250 μm, coated with a 1:1 mixture of PLG microspheres and salt (63–106 μm), and pressed into a salt-lined aluminum mold. The sugar strands were used to create nine channels and the salt created a porous structure. The materials were then equilibrated with CO_2 gas at 800 psi in a custom-made pressure vessel. Bridges were cut into 1.15 mm sections and leached to remove salt porogen. The bridges were stored in a desiccator until use.

Virus loading into bridges

Bridges were disinfected in 70% ethanol and washed with sterile water. Bridges were then saturated with 2 μL of virus. After 2 min of incubation, sterile filter paper was touched to the surface of the bridge to remove excess moisture. This process was repeated with another 2 μL of virus. The bridges were stored on ice until use. Bridges were used within 3 h of coating with lentivirus to preserve viral activity. Lentivirus loading conditions included NT-3, IL-10, and IL-10+NT-3.

Mouse spinal cord hemisection

All animal procedures were approved and in accordance with the Institutional Animal Care and Use Committee at the University of Michigan. A hemisection model of SCI was performed on female C57BL/6 mice (6–8 weeks old, total $N = 60$; Jackson Laboratories, Bar Harbor, ME) as previously described.[5] After administration of bupivacaine (0.8 mL/kg), a laminectomy was performed at C5 to allow for a 1.15 mm lateral hemisection on the left side of the spinal cord for bridge implantation. The C5 lateral hemisection causes deficits in the left forelimb function. The injury site was covered using Gelfoam (Pfizer, New York, NY) followed by suturing together of the muscle and stapling of skin. Postoperative care consisted of administration of enrofloxacin (2.5 mg/kg; daily for 2 weeks), buprenorphine (0.1 mg/kg; twice daily for 3 days), and lactated Ringer's solution (5 mL/100 g; daily for 5 days). Bladders were expressed twice daily until function recovered. No mice were lost using this injury model.

Western blot

Spinal cord tissues ($n = 4$/group, total $N = 12$) were collected at 2 weeks postinjury (wpi) and lysed with RIPA buffer (Thermo Fisher, Waltham, MA) supplemented with Halt Protease Inhibitor Cocktail (Thermo Fisher). The lysate was then sonicated and centrifuged. The supernatant was added with 2×Lammeli buffer (Biorad, Hercules, CA) and boiled for 5 min at 95°C. Samples were run on a 4–15% gradient sodium dodecyl sulfate–polyacrylamide gel electrophoresis (SDS-PAGE) gel (BioRad) and proteins were transferred to 0.45 μm nitrocellulose membranes. After blocking with BLOK Casein (G-Biosciences, St. Louis, MO), proteins were probed with primary antibodies against rabbit anti-IL-10 (Abcam, Cambridge, United Kingdom), rabbit anti-NT3 (Abcam), and rabbit anti-β actin (CST, Danvers, MA). The proteins were detected by chemiluminescence (Clarity Substrate; Thermo Fisher). Quantification was performed with ImageJ (NIH, Bethesda, MD).

Immunohistochemistry and quantitative analysis nerve regeneration and myelination

Spinal cords ($n = 6$/group, $N = 24$) were extracted 12 weeks after SCI and flash frozen in isopentane. For immunofluorescence, spinal cord segments were embedded in Tissue Tek O.C.T. Compound (Sakura Finetek, Torrance, CA) with 30% sucrose. Cords were cryosectioned transversely into 12 μm thick sections. Antibodies against the following antigens were used for immunofluorescence: F4/80 (Abcam), Arginase 1 (Arg1; Santa Cruz Biotech, Dallas, TX), neurofilament 200 (NF-200; Sigma-Aldrich), myelin

basic protein (MBP; Santa Cruz Biotech), and protein-zero myelin protein (P0; Aves Labs, Tigard, OR). Red fluorescent protein was imaged at 488 nm without added antibodies. Tissues were imaged on an Axio Observer Z1 (Zeiss, Oberkochen, Germany) using a 10×/0.45 or 20×/0.75 M27 apochromatic objective and an ORCA-Flash 4.0 V2 Digital CMOS camera (C11440-22CU; Hamamatsu Photonics, Hamamatsu City, Shizuoka, Japan).

For quantification of macrophage phenotypes, nine 12 μm thick transverse tissues were randomly selected from each animal ($n = 6$/group, $N = 24$). All immunopositive cell events were counterstained with Hoechst 33342 to indicate cell nuclei. F4/80$^+$ cells and F4/80$^+$/arginase1$^+$ (Arg1$^+$) were quantified to determine proinflammatory macrophages and noninflammatory macrophages, respectively. Immunopositive cells were counted within the bridge area by two blinded researchers independently. Costaining for multiple markers was assessed by evaluating overlap of different channels in ImageJ (NIH, Bethesda, MD).

To assess the numbers of regenerated and myelinated axons within the PLG bridge area, NF-200 was used to identify axons, NF-200$^+$/MBP$^+$ to determine the number of myelinated axons, and NF-200$^+$/MBP$^+$/P0$^+$ to determine the amount of myelin derived from infiltrating Schwann cells.[20] Twenty-four tissues distributed between conditions were counted by two blinded counters to calibrate software for automated counting as previously described.[2,22,23,26] In brief, images were imported into MATLAB (Mathworks, Natick, MA) and the area of the tissue section corresponding to PLG bridge was outlined. A Hessian matrix was created by convolution filtering using second derivative of the Gaussian function in the x, y, and xy directions. The matrix uses local image intensities variations to define continuous structures of axons. After filtering, positive NF-200 events were identified by intensity thresholding, single pixel events were removed, and the number of continuous objects identified to ensure high branching axons were counted as a single object. For calibration, the software outputs a matrix of predicted axon counts based on filtering parameters input by the user. These values were directly compared with manual counts for the 24 tissues used for calibrating the software. The appropriate filter size and threshold sensitivity were selected based on the lowest mean percentage error between the manual and automated counts. For these studies, the mean percentage error was 3%. Once calibration was complete, nine tissue sections per animal ($n = 6$/group, $N = 24$) were quantified. To obtain axon densities, total NF-200 counts were divided by the area of the PLG bridge. MBP and P0 events were identified similarly as described previously. NF200 objects containing pixel locations overlapping with positive MBP or P0 staining were counted and compared with total NF200 counts to determine percentages of axons populations.

Behavioral analysis

The ladder beam walking task was used to evaluate locomotor recovery over a period of 12 weeks post-SCI as previously described for all conditions ($n = 12$/group, $N = 48$).[27] In brief, animals were trained to walk across a ladder beam of 50 rungs into an enclosure over the course of 2 weeks before injury. Baseline scores were determined to

separate animals in equal groups before SCI. The mice were tested at 2, 4, 8, and 12 weeks. Observations and ladder beam scoring were performed by two blinded observers for three trials per animal. The C5 lateral hemisection causes deficits in left forelimb function. Therefore, animals were scored by average left forepaw full placements on the ladder beam during the task.

Thermal hyperalgesia

Cold sensitivity was assessed by acetone evaporative cooling over a period of 12 weeks post-SCI as previously described ($n = 12$/group, $N = 48$).[28] Through a mesh floor, five applications of acetone were applied to the bottom of the left and right forepaw. Each application was separated by at least 5 min. Individual responses were scored based on lifting, licking, or shaking of the forepaw that continued past the initial application. Scores were averaged over the 10 applications between left and right forepaws to yield a percentage of positive responses. The mice were tested at 2, 4, 8, and 12 weeks.

Statistical analysis

For single comparisons, statistical significance between groups was determined by one-way analysis of variance (ANOVA) with Tukey's *post hoc*. For multiple comparisons, statistical significance between groups was determined by two-way ANOVA with Tukey's *post hoc*. All statistics test significance using an α value of 0.05. For all graphs: a, b, c denotes $p < 0.05$ compared with Blank control, d and e denotes $p < 0.05$ compared with NT-3 condition, and f denotes $p < 0.05$ compared with IL-10 condition. Error bars represent standard error in all figures. Prism 7 (GraphPad Software, La Jolla, CA) software was used for all data analysis.

Data availability

The datasets generated during and/or analyzed during the current study are available from the corresponding author on reasonable request.

Results

Bicistronic vectors conserve IL-10 and NT-3 production in vivo

We initially assessed protein levels following expression from the lentivirus with a single construct and also the bicistronic construct (Fig. 1). Bridges were implanted into mice and explanted at 2 wpi. This time point was selected based on previous studies using bioluminescence imaging that demonstrates robust transgene expression.[19] The proteins used in these studies are human that enabled differentiation of the IL-10 and NT-3 produced by our constructs from the mouse proteins. No significant difference in protein expression was observed between single constructs or the bicistronic construct. Furthermore, for the bicistronic construct, no significant difference in protein expression was observed between the first gene, IL-10, and the second gene, NT-3.

### IL-10 delivery increases anti-inflammatory macrophages

We next investigated the macrophage population in the bridge at 12 wpi (Fig. 2), as this population could be influenced by the cytokine and neurotrophin expression. This analysis was performed at 12 wpi to analyze the chronic infiltration and phenotype of macrophages. We observed most of the macrophages as the injury were localized to the bridge and not the surrounding tissue (Fig. 2A). The macrophages in the bridge were evenly distributed and were observed in all conditions at similar densities (Fig. 2F). For these studies, proregenerative macrophages were assessed by colocalization of F4/80 and Arg (Fig. 2G). A significant threefold increase ($p < 0.05$) in the density of regenerative macrophages was observed for conditions with expression of IL-10 compared with the Blank and NT-3 conditions. Differences among these conditions were also significant for the percentage of proregenerative macrophages. Of note, 31% and 26% of F4/80$^+$ macrophages were regenerative for IL-10 and IL-10+NT-3 conditions, respectively, a twofold increase over Blank and NT-3 conditions (12% and 14%) (Fig. 2H).

Delivery of IL-10+NT3 enhances axonal growth into bridges

The extent of axonal elongation into the bridge was subsequently analyzed, which reflects the impact of expressing the factors on the capacity of the environment to promote regeneration (Fig. 3). Axons were observed throughout the bridge in all conditions. Axons in treatment groups appeared longer and more diffuse, whereas axons in the control condition appeared bundled and shorter in length (Fig. 3A–D). NT-3 and IL-10 delivery did not significantly increase axonal density compared with the control. However, combined
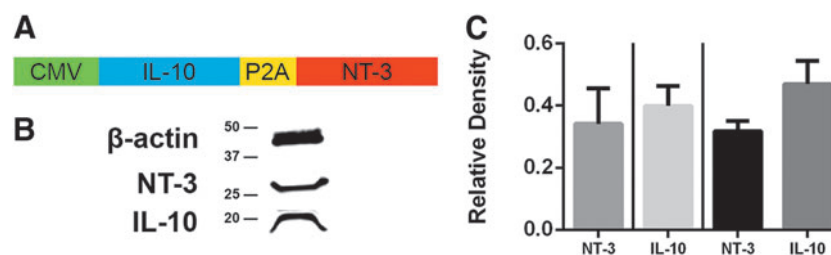
FIG. 1. Bicistronic vectors conserve IL-10 and NT-3 production *in vivo*. **(A)** Bicistronic lentiviral vector for delivery of IL-10+NT-3. **(B)** Western blotting was used to show protein levels of NT-3 (27 kDa) and IL-10 (21 kDa). **(C)** Relative densities of single lentiviral constructs and bicistronic construct of IL-10 and NT-3 relative to B-actin show no significant difference in protein expression for all comparisons ($p = 0.65$). Left of line are relative densities of single constructs and right of line is the bicistronic construct. Data are presented as mean ± SEM. $n = 4$ per group. SEM, standard error of the mean.
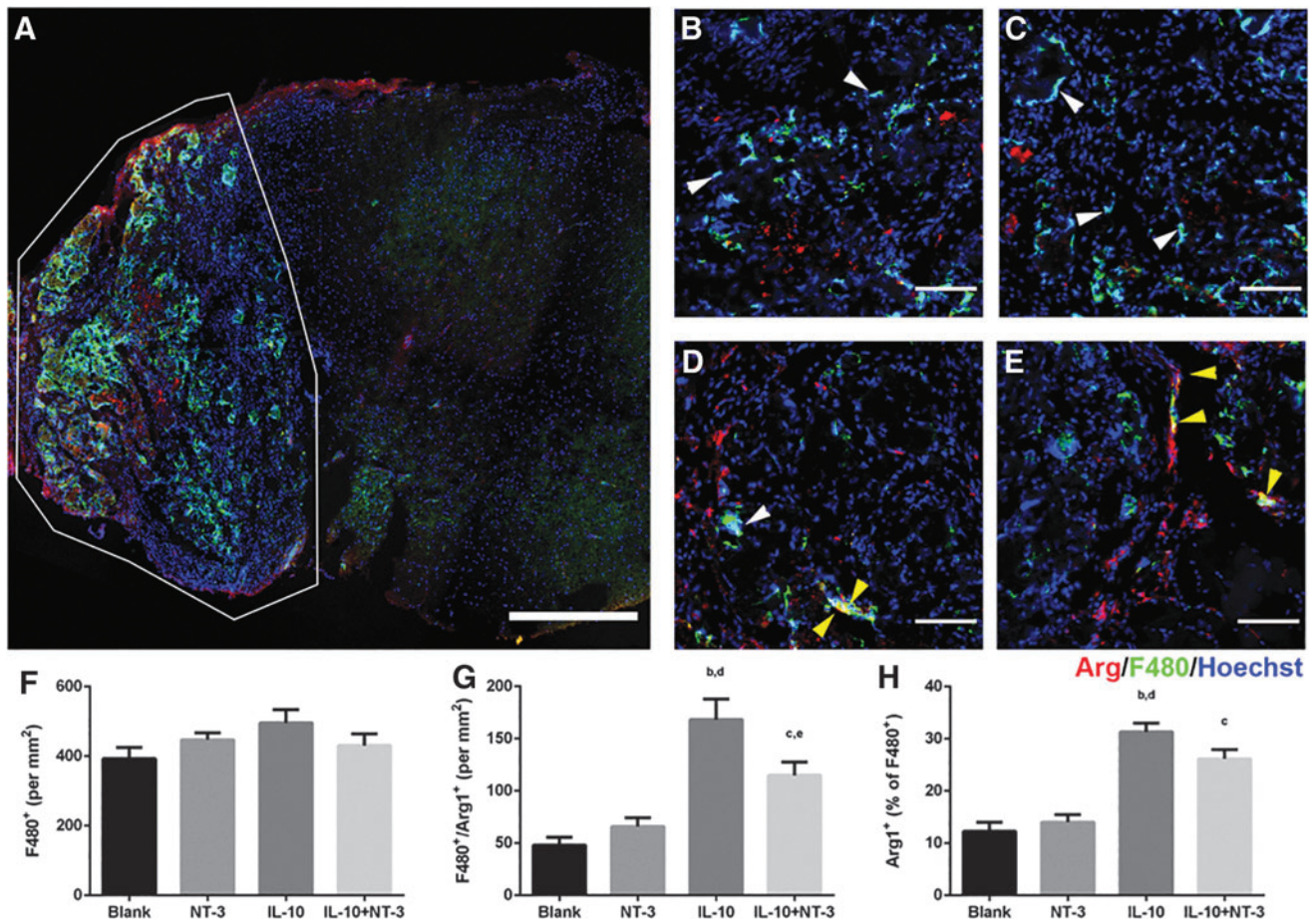
FIG. 2. IL-10 promotes anti-inflammatory macrophages. **(A)** Representative image of bridge implantation into spinal cord at 12 weeks postinjury. *Red* identifies arginase, *green* identifies F480, and *blue* identifies Hoechst. *White border* denotes bridge area. Scale: 500 µm. Macrophage density of **(B)** Blank (ctrl), **(C)** NT-3, **(D)** IL-10, and **(E)** IL-10+NT-3 from bridge implants. *White arrows* denote F480$^+$ macrophages. *Yellow arrows* denote F480$^+$/Arg$^+$ macrophages. Scale: 100 µm. **(F)** Macrophage density in bridge implants. Density **(G)** and percentage **(H)** of anti-inflammatory macrophages in bridge implants. "a, b, c" denotes $p < 0.05$ compared with Blank (ctrl), "d and e" denotes $p < 0.05$ compared with NT-3 condition, and "f" denotes $p < 0.05$ compared with IL-10 condition. Data are presented as mean ± SEM. $n = 6$ per group.

delivery of IL-10+NT-3 produced a significant increase of axonal density compared with all other conditions (Fig. 3E).

IL-10+NT-3 delivery promotes myelination of regenerating axons

Myelination of axons is necessary for signal propagation in the spinal cord, and myelinated axons (NF200$^+$/MBP$^+$) were observed throughout the bridges for all conditions (Fig. 4). Significantly more myelinated axons were observed in the IL-10 condition compared with the Blank bridge. IL-10+NT-3 delivery resulted in significantly more myelinated axons compared with Blank and NT-3 conditions (Fig. 4E). No significant difference was observed in the percentage of myelinated axons across the conditions, with levels at ∼27% of total axons (Fig. 4F).

Myelinated axons were subdivided into oligodendrocyte-derived myelin (NF200$^+$/MBP$^+$/P0$^-$) and Schwann cell-derived myelin (NF200$^+$/MBP$^+$/P0$^+$) (Fig. 5) to determine their relative contribution to total myelination. A significant twofold increase in oligodendrocyte-derived myelin density was observed for IL-10+NT-3 compared with Blank and

NT-3 conditions (Fig. 5E). IL-10 delivery resulted in a significant increase of oligodendrocyte myelin compared with the control. However, no significant difference in density of Schwann cell-derived myelin was observed across all conditions (Fig. 5F).

IL-10+NT-3 improves forelimb locomotor recovery

The ladder beam task was used to evaluate functional motor recovery of the left forelimb to determine if the observed regeneration correlated with an increase in function (Fig. 6A). A significant functional improvement was observed for all conditions compared with Blank. Furthermore, a significant increase in functional recovery was obtained with IL-10+NT-3 delivery compared with all other conditions at 12 wpi. Of interest, a greater prolonged improvement over time was observed for IL-10+NT-3 condition compared with other conditions. IL-10 and NT-3 delivery were similar in functional recovery; however, codelivery produced a significant additive effect in locomotor recovery.

We also assessed cold hypersensitivity using the acetone test to identify any potential negative effects that may be
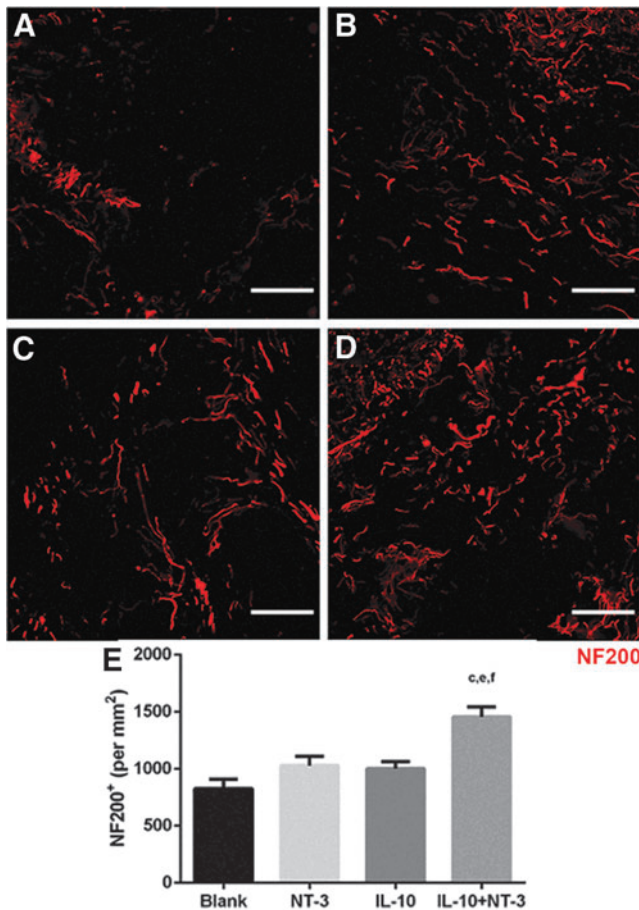
FIG. 3. IL-10+NT-3 delivery promotes axonal growth at 12 wpi. Axonal growth into bridge implants delivering **(A)** Blank (ctrl), **(B)** NT-3, **(C)** IL-10, or **(D)** IL-10+NT-3. Scale: 100 μm. **(E)** Axon density in bridge implants. ''a, b, c'' denotes $p < 0.05$ compared with Blank (ctrl), ''d and e'' denotes $p < 0.05$ compared with NT-3 condition, and ''f'' denotes $p < 0.05$ compared with IL-10 condition. Data are presented as mean ± SEM. $n = 6$ per group. *Red* identifies NF200. NF200, neurofilament 200; wpi, weeks postinjury.

associated with combined delivery (Fig. 6B). IL-10 delivery alone reduced cold hypersensitivity compared with all other conditions. NT-3 delivery alone exacerbated hypersensitivity compared with all conditions. The combined expression of IL-10+NT-3 led to increased hypersensitivity compared with IL-10 alone, yet decreased hypersensitivity relative to Blank and NT-3 conditions.

As a final analysis, we investigated the association of tissue recovery characteristics with forelimb locomotor function recovery (Fig. 7). The values for axon density (Fig. 7A), myelinated axon density (Fig. 7B), oligodendrocyte-derived myelinated axon density (Fig. 7C), and Schwann cell-derived myelinated axon density (Fig. 7D) were plotted against the ladder beam score for each animal. The oligodendrocyte myelinated axon density was positively correlated with functional recovery ($r = 0.59$, $p < 0.01$). This relationship also segments animals by condition along the interpolated linear fit line. This relationship was the only significant connection between tissue characteristics and functional recovery.

Discussion

The spinal cord environment lacks sufficient factors that promote regeneration and has an abundance of factors that inhibit regeneration.[9] We have developed multichannel PLG bridges that can promote nerve regeneration by both acting as a physical guide and serve as a platform for gene therapy vector delivery. The bridges are acellular at implantation, thus any cells, extracellular matrix, or proteins present at the time of extraction originate from the host tissue. Similarly, axons observed inside the implant represent either regenerating injured axons or sprouting of new axons from spared or contralateral tissue. This bridge provides a defined space for histological analysis, analysis of cell populations at and near the lesion site, and treatment outcomes. The bridge has an architecture that supports regeneration by combining microporosity for cellular infiltration with channels that direct axonal elongation along the major axis of the cord. These bridges can also be seeded with recombinant lentiviral particles containing genes of interest for subsequent cellular transduction. Unlike other viral vectors, lentivirus does not influence the phenotype of progenitors[29] or cause significant inflammation.[30] Lentiviral vector physical properties are also independent of the gene of interest, which enables delivery of multiple vectors encoding distinct inductive factors without modification to the base biomaterial. Polycistronic lentiviral vectors can deliver multiple genes by the inclusion of self-cleaving 2A peptide sites between genes. This technology is useful and beneficial to target multiple barriers to spinal cord regeneration by inducing the expression of multiple proteins simultaneously. The genes being used in this study were chosen because each addresses a distinct aspect of the inhibitory microenvironment around the injury site. NT-3 enhances axon elongation and neuroprotection of regenerating and spared axons.[19,31,32] IL-10 is largely responsible for dampening and resolving the immune response toward restoring homeostasis.[13,33,34] This research builds upon the success of the multiple channel PLG bridges by delivering two distinct transgenes alone and in combination. The goal of this investigation was to activate growth promoting cues while attenuating growth inhibitory cues to observe additive effects on spinal cord regeneration.

Macrophage infiltration into bridges was similar across experimental conditions delivering, yet transgene expression altered the macrophage phenotype. Macrophage exists on a spectrum of inflammatory to regenerative phenotypes; we have previously shown that Arg1^{+} macrophages have a regenerative phenotype in SCI.[11,23] We have previously shown that regenerative macrophages can be assessed by colocalization of F4/80[+] and Arg1^{+}.[23,35] The early phase of the regenerative response after SCI relies on proinflammatory macrophages, which participate in recruitment of immune cells and clearance of cell debris. Subsequently, these macrophages move toward to a proregenerative phenotype to coordinate cell differentiation and tissue reconstruction. Dysregulation of the transition from proinflammatory to proregenerative hampers regenerative success and tissue recovery.

In the central nervous system microglia and macrophages express several neurotrophins and their receptors, allowing them to act both as sources and targets creating a feedback loop that can modulate proliferation and morphology of axons.[36] Neurotrophins impact immune cell function in
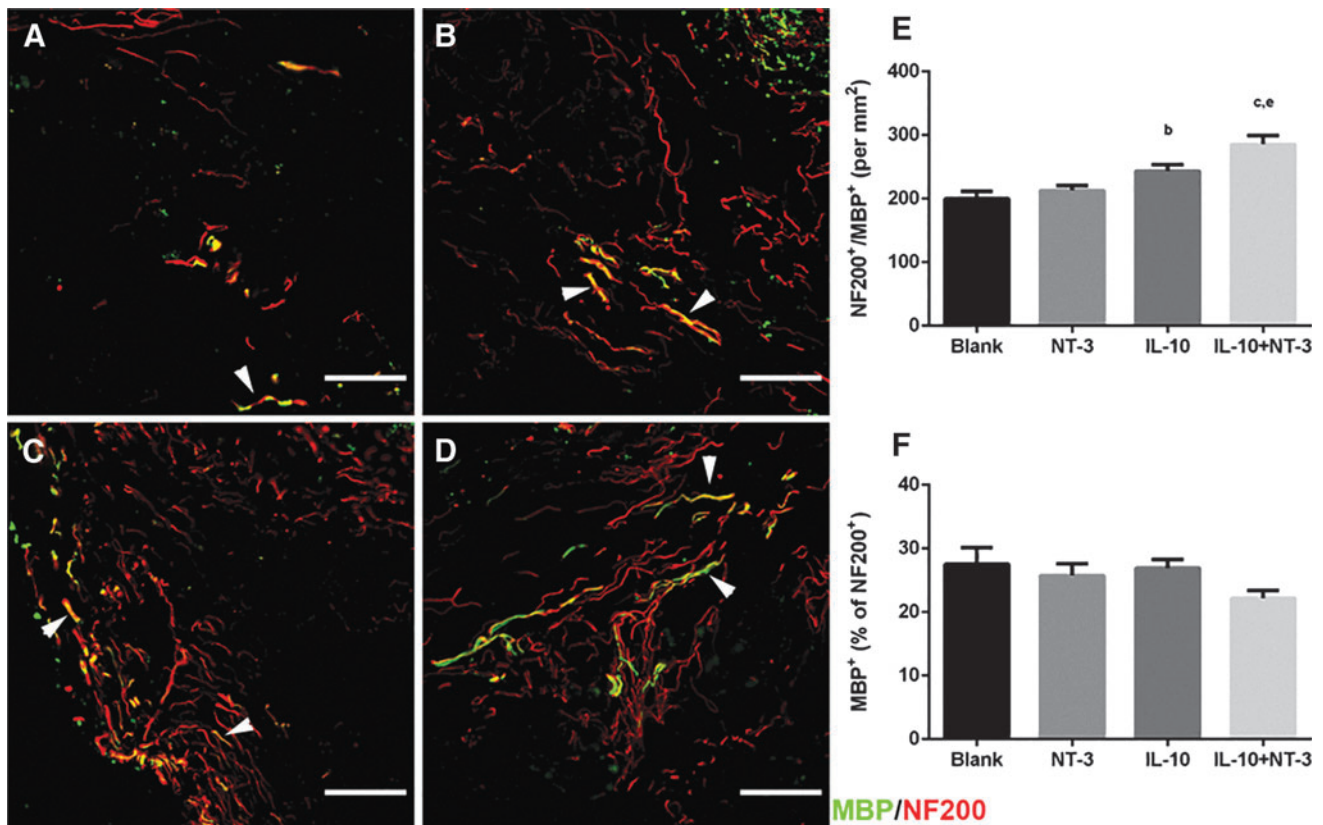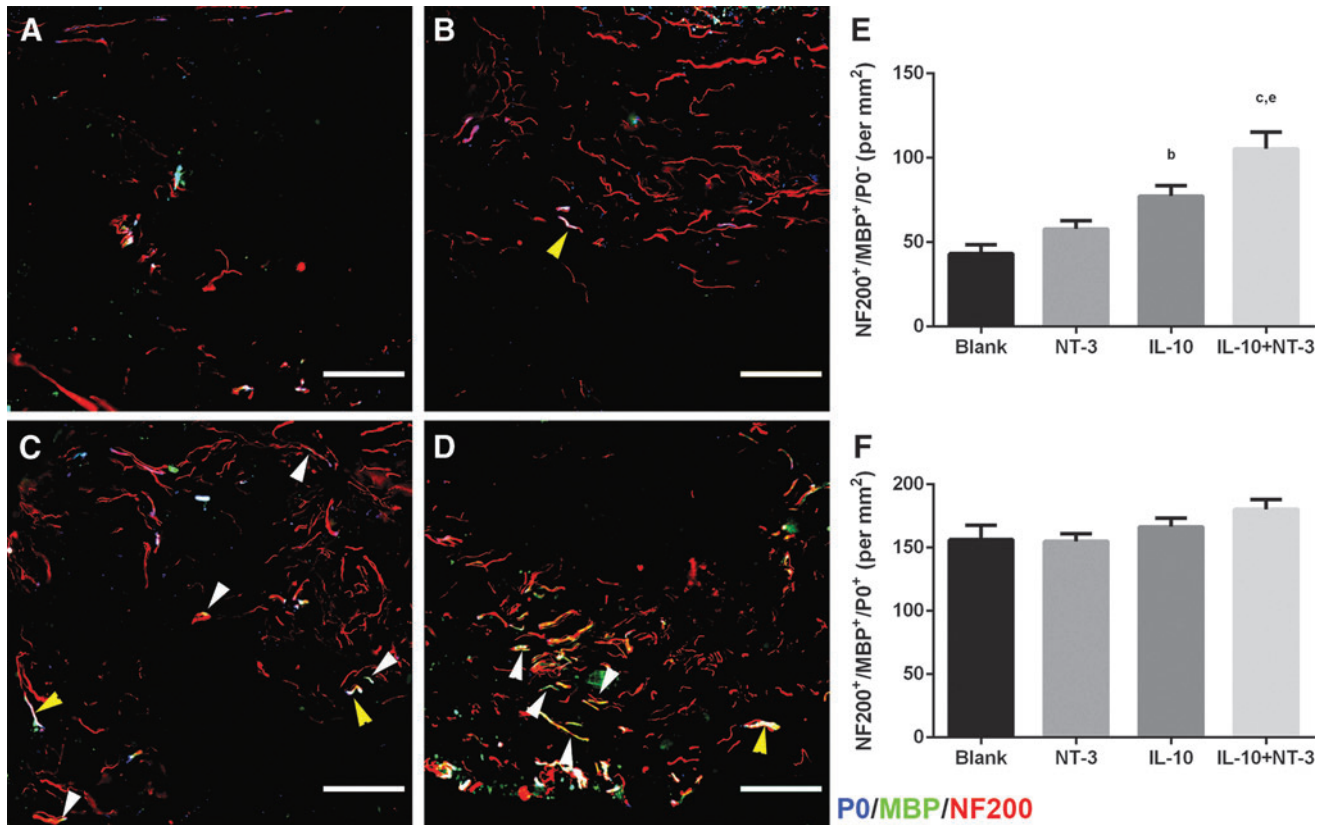
FIG. 4. IL-10+NT-3 delivery promotes myelination of regenerating axons at 12 wpi. Axon myelination from bridge implants delivering **(A)** Blank (ctrl), **(B)** NT-3, **(C)** IL-10, or **(D)** IL-10+NT-3. *White arrows* denote myelinated axons. Scale: 100 μm. Density **(E)** and **(F)** percentages of myelinated axons in bridge implants. ''a, b, c'' denotes $p < 0.05$ compared with Blank (ctrl), ''d and e'' denotes $p < 0.05$ compared with NT-3 condition, and ''f'' denotes $p < 0.05$ compared with IL-10 condition. Data are presented as mean ± SEM. $n = 6$ per group. *Red* identifies NF200 and *green* identifies MBP. MBP, myelin basic protein.

varying ways. Brain-derived neurotrophic factor stimulates microglial proliferation, whereas NT-3 can stimulate phagocytic activity of microglial cells *in vitro* and upregulation of nitric oxide production.[36–38] NGF can also act directly on microglial cells by promoting chemotactic migratory activity, potentially contributing to recruitment of additional immune cells at injury sites.[39] Neurotrophins, including NT-3, have been suggested as modulating monocyte chemotaxis without altering their production of inflammatory cytokines.[40] NGF can act directly on microglia and shift them toward a neuroprotective phenotype.[39] In these studies, we did not observe an anti-inflammatory effect of NT-3 on macrophage activity. IL-10 delivery alone produced ∼31% of regenerative macrophages, but when combined with NT-3, this percentage decreased to 26%. This difference was not significant. IL-10 has been extensively revered as an anti-inflammatory cytokine capable of shifting the phenotype of macrophages.[22,41–45] and these studies support the previous findings.

A trend of increased axons for NT-3 and IL-10 compared with Blank, yet the combination of IL-10+NT-3 produced an additive effect for axonal outgrowth. Axonal outgrowth can be impacted by delivery of NT-3 and IL-10 individually[19,22,23]; however, in our studies, these individual factors did not substantially impact axon density relative to control. This observation could reflect differences in the C5 lateral hemisection model compared with previous reports in thoracic hemisection.

For example, a larger number of propriospinal neurons are present in the cervical spinal cord than the thoracic spinal cord, with intrinsic differences also reported for growth factors, cell surface receptors, apoptosis, axonal regeneration, neuroprotection, and cell survival.[46–49] Our results indicate that the combined expression of IL-10 and NT-3 does significantly enhance axon density at the cervical hemisection. This synergy could be related to the sparing of axons by IL-10 and the neurotrophic effects of NT-3. Effectively, the greater survival of axons by IL-10 leads to an increase in the number of axons that can regenerate into the bridge.

An increase in myelinated axons for IL-10+NT-3 delivery, notably with oligodendrocyte myelinated axons was observed. Oligodendrocyte myelin is necessary to support saltatory conduction and prevent axon degeneration.[50] Oligodendrocyte proliferation is not altered by NT-3; NT-3 exposure *in vitro* lead to significantly more MBP production by oligodendrocytes through an unknown post-transcriptional mechanism.[51,52] Some evidence suggests that NT-3 weakly induces the maturation of neural precursor cells into myelinating oligodendrocytes[53]; yet other reports have shown NT-3 promotes quiescence or even Schwann cell differentiation of neural precursor cells.[20,54–56] These differences could indicate concentration-dependent effects or vary with surrounding interactions with other factors. We observed that IL-10 delivery had significantly more

FIG. 5. IL-10+NT-3 delivery promotes oligodendrocyte myelination of regenerating axons at 12 wpi. Source of myelination from bridge implants delivering **(A)** Blank (ctrl), **(B)** NT-3, **(C)** IL-10, or **(D)** IL-10+NT-3. *White arrows* denote oligodendrocyte myelinated axons. *Yellow arrows* denote Schwann cell myelinated axons. Scale: 100 μm. **(E)** Density of oligodendrocyte myelinated axons. **(F)** Density of Schwann cell myelinated axons. ''a, b, c'' denotes $p < 0.05$ compared with Blank (ctrl), ''d and e'' denotes $p < 0.05$ compared with NT-3 condition, and ''f'' denotes $p < 0.05$ compared with IL-10 condition. Data are presented as mean ± SEM. $n = 6$ per group. *Red* identifies NF200, *green* identifies MBP, and *blue* identifies p-zero (P0).

oligodendrocyte-derived myelin relative to control. IL-10 polarization of immune cells enhances the ability of neural precursor cells to promote oligodendrocyte differentiation and supports mature oligodendrocyte survival by promoting an anti-inflammatory environment rather than acting on

neural precursor cells directly.[57] Our results are consistent with this observation that IL-10 promoted the survival of myelinating oligodendrocytes, which can synergize with the expression of NT-3 to potentiate their myelin production to ensheath more axons. This mechanism has been suggested in
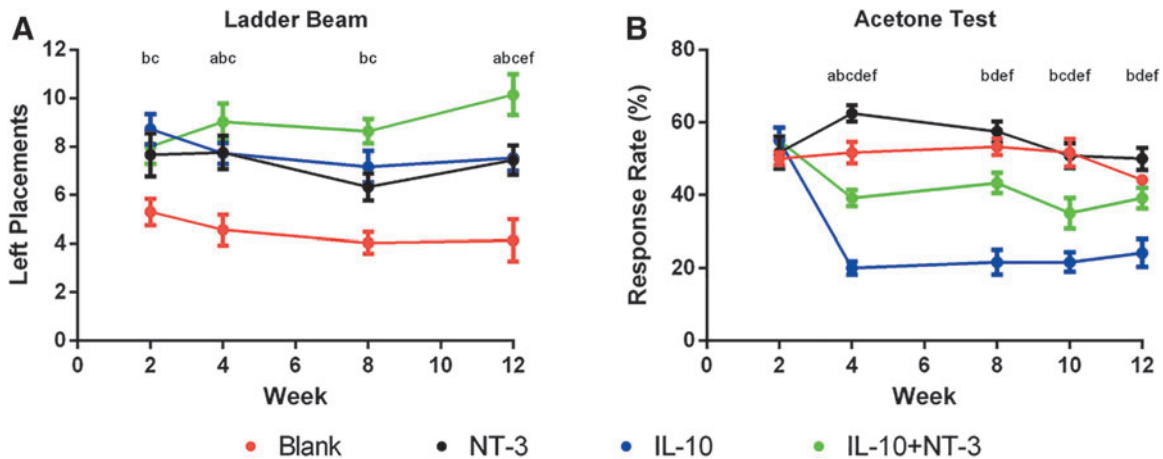
FIG. 6. IL-10+NT-3 enhances functional recovery and causes some cold hypersensitivity. **(A)** Ladder beam task was evaluated over 12 weeks postbridge implantation. **(B)** Acetone cold hypersensitivity test was evaluated over 12 weeks postbridge implantation. ''a, b, c'' denotes $p < 0.05$ compared with Blank (ctrl) for NT-3, IL-10, and IL-10+NT-3, respectively, ''d and e'' denotes $p < 0.05$ compared with NT-3 for IL-10 and IL-10+NT-3 respectively, and ''f'' denotes $p < 0.05$ compared with IL-10 for IL-10+NT-3. Data are presented as mean ± SEM. $n = 12$ per group.
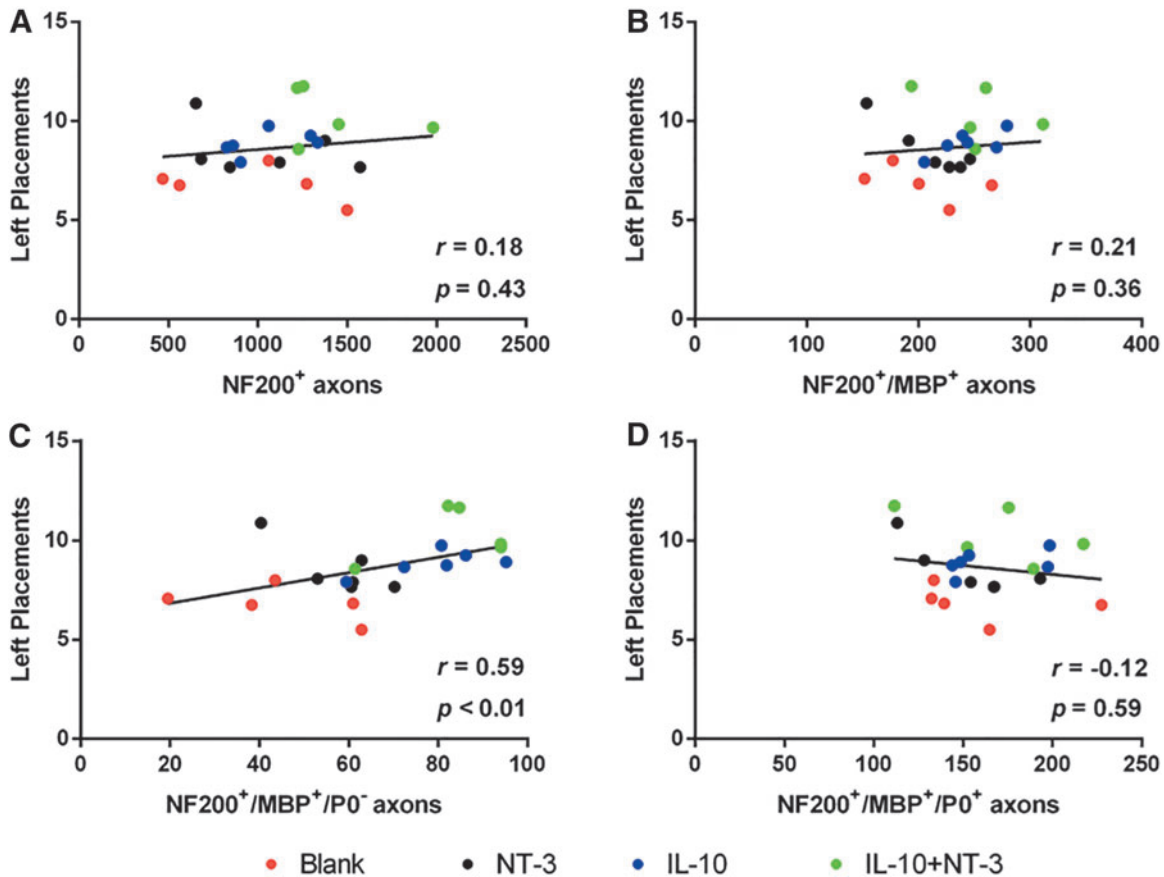
FIG. 7. Functional recovery is correlated to oligodendrocyte myelinated axon density. Ladder beam left forelimb placements correlated with **(A)** axon density, **(B)** myelinated axon density, **(C)** oligodendrocyte myelinated axon density, and **(D)** Schwann cell myelinated axon density. *R* value denotes Spearman's rank correlation coefficient. *p* Values denote significance from zero slope. $n = 12$ per group.

other work combining IL-10 and NT-3 delivery for treatment of multiple sclerosis.[58] We did not observe an increase in oligodendrocyte myelination for NT-3 delivery alone, possibly because of lack of surviving oligodendrocytes and weak effects of NT-3 on their proliferation and differentiation.[53]

Oligodendrocyte myelination significantly correlated with increased functional recovery. We assessed locomotor recovery on the ladder beam walking task over the course of 12 weeks. All treatment conditions had significant improvements in functional recovery relative to control, yet IL-10+NT-3 delivery was substantially improved relative to all other conditions. A significant correlation between ladder beam score and oligodendrocyte myelinated axon density was observed, suggesting that oligodendrocyte myelination of axons is a limiting step in functional recovery for our model. The functional benefits of oligodendrocyte myelin versus Schwann cell myelin have been debated in the literature, yet any conclusion remains nebulous. Some reports suggest oligodendrocyte myelin is not necessary in spontaneous functional recovery[59]; however, prolonged recovery as seen in these studies may require oligodendrocyte myelin for restoration of function. The various injury models may differentially impact oligodendrocytes as oligodendrocyte have been seen as less important in contusion models.[59] Our hemisection model severs and removes existing axons and cells in the lesion, while contusion models retain the damaged tissue.

A decrease in hypersensitivity was observed with IL-10 delivery, whereas NT-3 delivery alone increased hypersensitivity. IL-10 has been shown to ameliorate neuropathic pain but the role played by neurotrophins and NT-3 has been nebulous.[35] NT-3 can be involved in a long-term change of neuronal excitability.[60] NT-3 also promotes an extensive growth of lesioned axons in the dorsal columns that contain mostly sensory projections. Furthermore, the effects of NT-3 on neuropathic pain may be concentration or receptor dependent.[61–63] Our results suggest NT-3 exacerbates neuropathic pain. However, there exists a tradeoff of positive and negative effects. We observed the highest degree of functional recovery when combining IL-10+NT-3, yet we also observed increased neuropathic pain compared with IL-10 alone.

Conclusion

Overall our results show that the combination of IL-10+NT-3 enhanced axonal growth and oligodendrocyte myelinated axon density, and with increased locomotor functional recovery compared with IL-10 or NT-3 alone. Hypersensitivity with the combination was increased compared with IL-10 alone yet decreased relative to NT-3 alone. Furthermore, a positive correlation was observed between oligodendrocyte myelinated axon density and functional recovery, suggesting oligodendrocyte myelination as a

target to further improve functional recovery. Polycistronic vectors provide a mechanism for expression of multiple transgenes that can simultaneously address multiple aspects that limit regeneration. Multichannel PLG bridges provide a growth supportive substrate and a platform to deliver bioactive agents and a defined space to investigate the SCI microenvironment and to assess the biological impact of treatments.

Disclosure Statement

No competing financial interests exist.

Funding Information

References

1. Foundation, C.A.D.R.A.C.F.D. One Degree of Separation: Paralysis and Spinal Cord Injury in the United States, 2009.
2. Smith, D.R., Margul, D.J., Dumont, C.M., et al. Combinatorial lentiviral gene delivery of pro-oligodendrogenic factors for improving myelination of regenerating axons after spinal cord injury. Biotechnol Bioeng 116, 155, 2019.
3. Dumont, C., Munsell, M., Carlson, M., Cummings, B., Anderson, A., and Shea, L. Spinal progenitor-laden bridges support earlier axon regeneration following spinal cord injury. Tissue Eng Part A 24, 1588, 2018.
4. Brazda, N., Estrada, V., Voss, C., Seide, K., Trieu, H.K., and Muller, H.W. Experimental strategies to bridge large tissue gaps in the injured spinal cord after acute and chronic lesion. J Vis Exp, e53331, 2016; DOI: 10.3791/53331.
5. Pawar, K., Cummings, B.J., Thomas, A., et al. Biomaterial bridges enable regeneration and re-entry of corticospinal tract axons into the caudal spinal cord after SCI: association with recovery of forelimb function. Biomaterials 65, 1, 2015.
6. Grulova, I., Slovinska, L., Blaško, J., et al. Delivery of alginate scaffold releasing two trophic factors for spinal cord injury repair. Sci Rep 5, 13702, 2015.
7. Zamani, F., Amani-Tehran, M., Latifi, M., Shokrgozar, M.A., and Zaminy, A. Promotion of spinal cord axon regeneration by 3D nanofibrous core-sheath scaffolds. J Biomed Mater Res A 102, 506, 2014.
8. Huang, J., Lu, L., Zhang, J., et al. Electrical stimulation to conductive scaffold promotes axonal regeneration and remyelination in a rat model of large nerve defect. PLoS One 7, e39526, 2012.
9. Bunge, M.B. Novel combination strategies to repair the injured mammalian spinal cord. J Spinal Cord Med 31, 262, 2008.
10. Golz, G., Uhlmann, L., Ludecke, D., Markgraf, N., Nitsch, R., and Hendrix, S. The cytokine/neurotrophin axis in peripheral axon outgrowth. Eur J Neurosci 24, 2721, 2006.
11. Kigerl, K.A., Gensel, J.C., Ankeny, D.P., Alexander, J.K., Donnelly, D.J., and Popovich, P.G. Identification of two distinct macrophage subsets with divergent effects causing either neurotoxicity or regeneration in the injured mouse spinal cord. J Neurosci 29, 13435, 2009.
12. Murray, P.J., and Wynn, T.A. Obstacles and opportunities for understanding macrophage polarization. J Leukoc Biol 89, 557, 2011.
13. Murray, P.J., and Wynn, T.A. Protective and pathogenic functions of macrophage subsets. Nat Rev Immunol 11, 723, 2011.
14. Porcheray, F., Viaud, S., Rimaniol, A.C., et al. Macrophage activation switching: an asset for the resolution of inflammation. Clin Exp Immunol 142, 481, 2005.
15. Ogden, C.A., Pound, J.D., Batth, B.K., et al. Enhanced apoptotic cell clearance capacity and B cell survival factor production by IL-10-activated macrophages: implications for Burkitt's lymphoma. J Immunol 174, 3015, 2005.
16. Mokarram, N., Merchant, A., Mukhatyar, V., Patel, G., and Bellamkonda, R.V., Effect of modulating macrophage phenotype on peripheral nerve repair. Biomaterials 33, 8793, 2012.
17. Boato, F., Hechler, D., Rosenberger, K., et al. Interleukin-1 beta and neurotrophin-3 synergistically promote neurite growth in vitro. J Neuroinflammation 8, 183, 2011.
18. Daneman, R., and Prat, A. The blood-brain barrier. Cold Spring Harb Perspect Biol 7, a020412, 2015.
19. Tuinstra, H.M., Aviles, M.O., Shin, S., et al. Multifunctional, multichannel bridges that deliver neurotrophin encoding lentivirus for regeneration following spinal cord injury. Biomaterials 33, 1618, 2012.
20. Thomas, A.M., Seidlits, S.K., Goodman, A.G., et al. Sonic hedgehog and neurotrophin-3 increase oligodendrocyte numbers and myelination after spinal cord injury. Integr Biol (Camb) 6, 694, 2014.
21. Liu, Z., Chen, O., Wall, J.B.J., et al. Systematic comparison of 2A peptides for cloning multi-genes in a polycistronic vector. Sci Rep 7, 2193, 2017.
22. Margul, D.J., Park, J., Boehler, R.M., et al. Reducing neuroinflammation by delivery of IL-10 encoding lentivirus from multiple-channel bridges. Bioeng Transl Med 1, 136, 2016.
23. Park, J., Decker, J.T., Margul, D.J., et al. Local immunomodulation with anti-inflammatory cytokine-encoding lentivirus enhances functional recovery after spinal cord injury. Mol Ther 26, P1756, 2018.
24. Li, J., Rickett, T.A., and Shi, R. Biomimetic nerve scaffolds with aligned intraluminal microchannels: a ''sweet'' approach to tissue engineering. Langmuir 25, 1813, 2009.
25. Thomas, A., Kubilius, L., Holland, S., et al. Channel density and porosity of degradable bridging scaffolds on axon growth after spinal injury. Biomaterials 34, 2213, 2013.
26. McCreedy, D.A., Margul, D.J., Seidlits, S.K., et al. Semi-automated counting of axon regeneration in poly(lactide co-glycolide) spinal cord bridges. J Neurosci Methods 263, 15, 2016.
27. Cummings, B.J., Engesser-Cesar, C., Cadena, G., and Anderson, A.J. Adaptation of a ladder beam walking task to assess locomotor recovery in mice following spinal cord injury. Behav Brain Res 177, 232, 2007.
28. Choi, Y., Yoon, Y.W., Na, H.S., Kim, S.H., and Chung, J.M. Behavioral signs of ongoing pain and cold allodynia in a rat model of neuropathic pain. Pain 59, 369, 1994.
29. Hughes, S.M., Moussavi-Harami, F., Sauter, S.L., and Davidson, B.L. Viral-mediated gene transfer to mouse primary neural progenitor cells. Mol Ther 5, 16, 2002.
30. Abdellatif, A.A., Pelt, J.L., Benton, R.L., et al. Gene delivery to the spinal cord: comparison between lentiviral, adenoviral, and retroviral vector delivery systems. J Neurosci Res 84, 553, 2006.
31. Wang, Q., and Green, S.H. Functional role of neurotrophin-3 in synapse regeneration by spiral ganglion neurons on inner hair cells after excitotoxic trauma in vitro. J Neurosci 31, 7938, 2011.
32. García-Alías, G., Petrosyan, H.A., Schnell, L., et al. Chondroitinase ABC combined with neurotrophin NT-3

secretion and NR2D expression promotes axonal plasticity and functional recovery in rats with lateral hemisection of the spinal cord. J Neurosci **31,** 17788, 2011.

33. Mosser, D.M. The many faces of macrophage activation. J Leukoc Biol **73,** 209, 2003.

34. Sindrilaru, A., Peters, T., Wieschalka, S., *et al.* An unrestrained proinflammatory M1 macrophage population induced by iron impairs wound healing in humans and mice. J Clin Invest **121,** 985, 2011.

35. Park, J., Decker, J.T., Smith, D.R., Cummings, B.J., Anderson, A.J., and Shea, L.D. Reducing inflammation through delivery of lentivirus encoding for anti-inflammatory cytokines attenuates neuropathic pain after spinal cord injury. J Control Release **290,** 88, 2018.

36. Barouch, R., Appel, E., Kazimirsky, G., and Brodie, C. Macrophages express neurotrophins and neurotrophin receptors: regulation of nitric oxide production by NT-3. J Neuroimmunol **112,** 72, 2001.

37. Zhang, J., Geula, C., Lu, C., Koziel, H., Hatcher, L.M., and Roisen, F.J. Neurotrophins regulate proliferation and survival of two microglial cell lines *in vitro*. Exp Neurol **183,** 469, 2003.

38. Sousa-Victor, P., Jasper, H., and Neves, J. Trophic factors in inflammation and regeneration: the role of MANF and CDNF. Front Physiol **9,** 1629, 2018.

39. Williams, K.S., Killebrew, D.A., Clary, G.P., Seawell, J.A., and Meeker, R.B. Differential regulation of macrophage phenotype by mature and pro-nerve growth factor. J Neuroimmunol **285,** 76, 2015.

40. Samah, B., Porcheray, F., and Gras, G. Neurotrophins modulate monocyte chemotaxis without affecting macrophage function. Clin Exp Immunol **151,** 476, 2008.

41. Dumont, C.M., Park, J., and Shea, L.D. Controlled release strategies for modulating immune responses to promote tissue regeneration. J Control Release **219,** 155, 2015.

42. Dumont, C.M., Margul, D.J., and Shea, L.D. Tissue engineering approaches to modulate the inflammatory milieu following spinal cord injury. Cells Tissues Organs **202,** 52, 2016.

43. Boehler, R.M., Kuo, R., Shin, S., *et al.* Lentivirus delivery of IL-10 to promote and sustain macrophage polarization towards an anti-inflammatory phenotype. Biotechnol Bioeng **111,** 1210, 2014.

44. Walter, M.R. The molecular basis of IL-10 function: from receptor structure to the onset of signaling. Curr Top Microbiol Immunol **380,** 191, 2014.

45. Verma, R., Balakrishnan, L., Sharma, K., *et al.* A network map of Interleukin-10 signaling pathway. J Cell Commun Signal **10,** 61 2016.

46. Siebert, J.R., Middleton, F.A., and Stelzner, D.J. Long descending cervical propriospinal neurons differ from thoracic propriospinal neurons in response to low thoracic spinal injury. BMC Neurosci **11,** 148, 2010.

47. Stelzner, D.J. Short-circuit recovery from spinal injury. Nat Med **14,** 19, 2008.

48. Siebert, J.R., Middelton, F.A., and Stelzner, D.J. Intrinsic response of thoracic propriospinal neurons to axotomy. BMC Neurosci **11,** 69, 2010.

49. Conta, A.C., and Stelzner, D.J. Differential vulnerability of propriospinal tract neurons to spinal cord contusion injury. J Comp Neurol **479,** 347, 2004.

50. Loers, G., Aboul-Enein, F., Bartsch, U., Lassmann, H., and Schachner, M. Comparison of myelin, axon, lipid, and immunopathology in the central nervous system of differentially myelin-compromised mutant mice: a morphological and biochemical study. Mol Cell Neurosci **27,** 175, 2004.

51. Coelho, R.P., Yuelling, L.M., Fuss, B., and Sato-Bigbee, C. Neurotrophin-3 targets the translational initiation machinery in oligodendrocytes. Glia **57,** 1754, 2009.

52. Yan, H., and Wood, P.M. NT-3 weakly stimulates proliferation of adult rat O1(-)O4(+) oligodendrocyte-lineage cells and increases oligodendrocyte myelination *in vitro*. J Neurosci Res **62,** 329, 2000.

53. Pöyhönen, S., Er, S., Domanskyi, A., and Airavaara, M. Effects of neurotrophic factors in glial cells in the central nervous system: expression and properties in neurodegeneration and injury. Front Physiol **10,** 486, 2019.

54. Delgado, A.C., Ferron, S.R., Vicente, D., *et al.* Endothelial NT-3 delivered by vasculature and CSF promotes quiescence of subependymal neural stem cells through nitric oxide induction. Neuron **83,** 572, 2014.

55. Silva-Vargas, V., and Doetsch, F. A new twist for neurotrophins: endothelial-derived NT-3 mediates adult neural stem cell quiescence. Neuron **83,** 507, 2014.

56. Assinck, P., Duncan, G.J., Plemel, J.R., *et al.* Myelinogenic plasticity of oligodendrocyte precursor cells following spinal cord contusion injury. J Neurosci **37,** 8635, 2017.

57. Dyck, S., Kataria, H., Alizadeh, A., *et al.* Perturbing chondroitin sulfate proteoglycan signaling through LAR and PTPsigma receptors promotes a beneficial inflammatory response following spinal cord injury. J Neuroinflammation **15,** 90, 2018.

58. Li, X., Zhang, Y., Yan, Y., *et al.* Neural stem cells engineered to express three therapeutic factors mediate recovery from chronic stage CNS autoimmunity. Mol Ther **24,** 1456, 2016.

59. Duncan, G.J., Manesh, S.B., Hilton, B.J., *et al.* Locomotor recovery following contusive spinal cord injury does not require oligodendrocyte remyelination. Nat Commun **9,** 3066, 2018.

60. Khan, N., and Smith, M.T. Neurotrophins and neuropathic pain: role in pathobiology. Molecules (Basel, Switzerland) **20,** 10657, 2015.

61. Bradbury, E.J., Khemani, S., Von King, R., Priestley, J.V., and McMahon, S.B. NT-3 promotes growth of lesioned adult rat sensory axons ascending in the dorsal columns of the spinal cord. Eur J Neurosci **11,** 3873, 1999.

62. Obata, K., Yamanaka, H., Dai, Y., *et al.* Contribution of degeneration of motor and sensory fibers to pain behavior and the changes in neurotrophic factors in rat dorsal root ganglion. Exp Neurol **188,** 149, 2004.

63. Siniscalco, D., Giordano, C., Rossi, F., Maione, S., and de Novellis, V. Role of neurotrophins in neuropathic pain. Curr Neuropharmacol **9,** 523, 2011.

Address correspondence to:
Lonnie D. Shea, PhD
Department of Biomedical Engineering
University of Michigan
1119 Carl A. Gerstacker Building
Ann Arbor, MI 48109-2099

E-mail: ldshea@umich.edu